Cell. Mol. Life Sci. (2014) 71:2547–2559
DOI 10.1007/s00018-013-1503-1

Cellular and Molecular Life Sciences

RESEARCH ARTICLE

Nucleolar localization and circadian regulation of Per2S, a novel splicing variant of the Period 2 gene

Daniele Avitabile · Licia Genovese · Donatella Ponti · Danilo Ranieri · Salvatore Raffa · Antonella Calogero · Maria Rosaria Torrisi

Received: 13 May 2013 / Revised: 26 September 2013 / Accepted: 17 October 2013 / Published online: 8 November 2013

Abstract In this work, we show for the first time that a second splicing variant of the core clock gene Period 2 (Per2), Per2S, is expressed at both the mRNA and protein levels in human keratinocytes and that it localizes in the nucleoli. Moreover, we show that a reversible perturbation of the nucleolar structure acts as a resetting stimulus for the cellular clock. Per2S expression and periodic oscillation upon dexamethasone treatment were assessed by qRT-PCR using specific primers. Western blot (WB) analysis using an antibody against the recombinant human PER2 (abRc) displayed an intense band at a molecular weight of ~55 kDa, close to the predicted size of Per2S, and a weaker band at the expected size of Per2 (~140 kDa). The antibody raised against PER2 pS662 (abS662), an epitope absent in PER2S, detected only the higher band. Immunolocalization studies with abRc revealed a peculiar nucleolar signal colocalizing with the nucleolar marker nucleophosmin, whereas with abS662 the signal was predominantly diffuse all over the nucleus and partially colocalized with abRc in the nucleolus. The analysis of cell fractions by WB confirmed the enrichment of PER2S and the presence of PER2 in the nucleolar compartment. Finally, a pulse (1 h) of actinomycin D (0.01 μg/ml) induced reversible nucleolar disruption, PER2S de-localization and circadian synchronization of clock and Per2S genes. Our work represents the first evidence that the Per2S splicing isoform is a clock component expressed in human cells localizing in the nucleolus. These results suggest a critical role for the nucleolus in the process of circadian synchronization in human keratinocytes.

Keywords Per2 · Per2 splicing variant · Actinomycin D · Nucleolus · Dexamethasone · Circadian clock

D. Avitabile and L. Genovese have contributed equally to this work.

Electronic supplementary material The online version of this article (doi:10.1007/s00018-013-1503-1) contains supplementary material, which is available to authorized users.

D. Avitabile (✉) · L. Genovese · D. Ranieri · S. Raffa · M. R. Torrisi
Department of Clinical and Molecular Medicine, Istituto Pasteur-Fondazione Cenci Bolognetti, Sapienza University of Rome, Via di Grottarossa 1035, 00189 Rome, Italy
e-mail: daniele.avitabile@uniroma1.it

D. Ponti · A. Calogero
Department of Medical-Surgical Science and Biotechnologies, Sapienza University of Rome, Corso della Repubblica 79, 04100 Latina, Italy

Introduction

Circadian rhythms are biological processes characterized by an oscillation of ~24 h. They represent a highly conserved and self-sustained time tracking system that allows the organism's physiology to be adjusted (entrained) to the environmental cues called zeitgebers (the most important of which is daylight). In mammals, the master circadian clock is localized in the suprachiasmatic nuclei of the hypothalamus where external stimuli are transduced into neurohormonal signals acting on the peripheral circadian systems (i.e., liver, heart and skin) [1].

At the molecular level, the circadian clock is regulated in both the SCN and the peripheral organs by a complex network of transcriptional/translational feedback loops. The positive limb of the main loop is generated by the heterodimerization of the transcription factor circadian locomotor output cycles kaput (CLOCK) and brain and muscle aryl hydrocarbon receptor nuclear translocator (ARNT)-like protein-1 (BMAL1), which bind to E-Box elements of

their target genes and activate their transcription. BMAL1/CLOCK heterodimer induces the expression of its own repressors belonging to the Period (Per1–2–3) or cryptochrome (Cry1–2) gene families. In the negative limb of the loop, PER and CRY proteins form a complex in the cytoplasm that migrates to the nucleus to directly inhibit BMAL1/CLOCK [2]. An additional feedback loop involving the nuclear retinoic orphan receptors ROR and REV-ERBα/β participates and stabilizes the molecular network controlling Bmal1 gene expression [3]. In addition, several post-translational modifications of clock proteins are essential to maintain the correct circadian period [4].

More than 10 % of the entire genome and 20 % of the soluble protein fraction have been shown to be circadianly regulated [5–7]. As a consequence, the circadian clock regulates many cellular processes including energy metabolism, redox balance, proliferation, cell cycle, apoptosis, senescence and stress response. An alteration of circadian rhythms results in an increased insurgence of pathological conditions including cancer [8–10].

The Period 2 (Per2) gene is an important component of the circadian system. In addition to its role in molecular clock resetting [11, 12], it has also been implicated in tumor suppression [13–18].

Per2 function is fine-tuned by complex post-translational regulations including phosphorylation [19–21], deacetylation [22], protein/protein interactions controlling its stability [23] and intracellular localization [24–26]. PER proteins shuttle continuously between the nucleus and cytoplasm, and this dynamism is critical in maintaining the correct pace of the circadian clock [27].

At the transcriptional level, the regulation of Per2 expression is tissue specific and influenced by multiple transcription factors in addition to Bmal1 [28–31].

Molecular components of the mammalian circadian system are highly redundant (i.e., Clock and Npas2, Bmal1 and Bmal2, Per1–3, etc.), and multiple splicing variants or different isoforms have been already reported for Bmal1 [32] and Per1 [33], respectively. Per2S is a second splicing variant of the human Per2 gene, annotated in GeneBank with the accession number AB012614; however, its expression in human cells has never been addressed before. In this report we hypothesized that Per2S could represent a new component of the molecular clock. We performed our study on the spontaneously immortalized human keratinocyte cell line (HaCaT) as well as on primary cultured normal human keratinocytes (NHK). HaCaT cells were chosen since they have physiological properties very close to NHK and share with this cell type a functional molecular clock [34, 35]. We demonstrated that Per2S is expressed at both the mRNA and protein levels in human keratinocytes and that it oscillates with a circadian period in response to the synchronizing agent dexamethasone (Dex). Interestingly, immunofluorescence assays and biochemical analysis of cell fractions indicate that PER2S is particularly enriched within the nucleolar compartment. Moreover, a single pulse (1 h) with a low dose of actinomycin D (ActD), which is known to selectively inhibit Polymerase I transcription with consequent de-localization of many nucleolar proteins in the nucleoplasmic compartment [36], was able to induce reversible PER2S nucleolar de-localization and circadian synchronization of clock genes. Our study suggests the existence of an important cross-talk between the molecular clock and the nucleolar function, which is mediated, at least in part, by the PER2S isoform. Our report opens new roads of investigation regarding the circadian clock and its connection with cellular pathophysiologic processes associated with nucleolar functions.

Materials and methods

Cells and treatments

The human keratinocyte cell line HaCaT [37] was cultured in Dulbecco's modified Eagle's medium (DMEM), supplemented with 10 % fetal bovine serum (FBS) plus antibiotics. Primary cultures of NHKs were derived from skin biopsies and maintained in Medium 154-CF (Cascade Biologics, Portland, OR, USA) supplemented with Human Keratinocyte Growth Supplement (HKGS, Cascade Biologics) plus antibiotics and Ca^{2+} 0.03 mM (Cascade Biologics Inc.).

To determine Per2 and Per2S mRNA half-lives ($t_{1/2}$), HaCaT cells were treated with 5 μg/ml ActD for 0, 1, 4 and 8 h at 37 °C [38]. To study the influence of nucleolar perturbation on molecular clock function, HaCaT cells were treated with 0.01 μg/ml ActD for 1 h and chased in full medium at 37 °C. Alternatively, ActD was kept in the medium for the duration of the experiment. Dimethyl sulfoxide (DMSO)-treated HaCaT cells were used as negative control.

To assess synchronization with Dex, HaCaT cells were cultured in DMEM + 10 % FBS plus antibiotics until subconfluence was reached. Cells were left overnight in serum starvation and treated with Dex 100 nM for 1 h. Soon after treatment, cells were washed with 2× PBS and left in starvation until the end of the time course. Ethanol (EtOH)-treated HaCaT cells were used as negative control.

Immunofluorescence studies and confocal microscopy

HaCaT cells were grown on coverslips, treated with ActD and processed for immunofluorescence after 1 h of treatment and 6 and 24 h after drug removal. ActD treated and control HaCaT cells were fixed with 4 % paraformaldehyde

in PBS for 30 min followed by treatment with 0.1 M glycine for 20 min and with 0.1 % Triton X-100 for an additional 5 min to allow permeabilization. All these steps were performed at 25 °C. Cells were then incubated for 1 h at 25 °C with the following primary antibodies: mouse monoclonal anti-Per2 (1:100 in PBS; 19-JS, Santa Cruz Biotechnology), rabbit polyclonal anti-pS662PER2 (1:100 in PBS; A1223, Assay biotech), rabbit polyclonal anti-NPM (1:500 in PBS; ab37659, Abcam), rabbit polyclonal anti-CLOCK (1:50 in PBS; CLO12-A, Alpha Diagnostics), goat polyclonal anti-CRY2 (1:100 in PBS; A-20, Santa Cruz Biotechnology) and rabbit polyclonal anti-Bmal1 (1:50 in PBS; ab93806, Abcam). The primary antibodies were visualized, after appropriate washing with PBS, using goat anti-mouse IgG-FITC (1:20 in PBS; Cappel), goat anti-rabbit IgG-Texas Red (1:200 in PBS; Jackson Immunoresearch Laboratories, West Grove, PA, USA) and rabbit anti-goat IgG-FITC (1:400 in PBS; Cappel) for 30 min at 25 °C. Nuclei were stained with DAPI (1:10,000 in PBS; Sigma). Coverslips were finally mounted with mowiol for observation.

Images were captured with the ApoTome System (Zeiss, Oberkochen, Germany) connected with an Axiovert200 inverted microscope (Zeiss); image analysis was then performed by the Axiovision software (Zeiss). Fluorescent signals and serial sectioning (*Z*-stack ~0.3 μm) were also scanned by confocal microscopy using a Zeiss LSM5 Pascal Laser scan microscope.

Isolation of cell fractions

The nucleolar extracts were prepared as follows: growing cells (10^7 cells per T75 flask) were washed in cold PBS and lysed in 5 ml of buffer containing 10 mM HEPES, pH 7.9, 1.5 mM $MgCl_2$, 10 mM KCl and 0.5 mM DTT [39]. Lysis was performed with a Dounce homogenizer until the nuclei appeared free of cytoplasmic components as assessed by phase microscopy. The nuclei were collected by centrifugation at 1,000 g for 5 min, resuspended in 3 ml of solution S1 (0.25 M sucrose, 25 mM $MgCl_2$) and centrifugated on a cushion of 3 ml sucrose solution S2 (0.35 M sucrose, 12.5 mM $MgCl_2$) at 1,500*g* for 5 min. The nucleoli were then isolated by sonication of the nuclear enriched fraction in solution S2 followed by a centrifugation on a 3-ml cushion of sucrose solution S3 (0.88 M sucrose, 12.5 mM $MgCl_2$) at 3,000*g* for 10 min. The pellet containing intact nucleoli was washed once in the S2 solution and finally resuspended in 0.5 ml of the S2 solution. All steps were performed at 4 °C in the presence of protease inhibitors (complete, Sigma).

For nuclear and cytosolic extracts, cells at 80 % of confluence were washed twice with PBS and incubated with NE1 buffer (10 mM Hepes pH 8.0, 1.5 mM $MgCl_2$, 10 mM KCl, 1 mM DTT) for 15 min at 4 °C. Cell homogenization was performed using a Dounce homogenizer, and the lysate was centrifuged at 12,000 rpm for 5 min at 4 °C. The nuclear pellet was resuspended in NE2 buffer (20 mM Hepes pH 8.0, 1.5 mM $MgCl_2$, 25 % glycerol, 420 mM NaCl, 0.2 mM EDTA, 1 mM DTT and 0.5 mM PMSF) and incubated for 30 min at 4 °C. Furthermore, the supernatant, representing the cytosolic fraction, was centrifuged for 5 min at 12,000 rpm and then diluted 1:4 with water.

Western blot

WB on cytoplasmic, nuclear and nucleolar fractions was performed loading 9 μg of protein for each fraction. Western blot on total cell lysates was performed loading 60 or 90 μg of protein extracts. The protein concentration of all extracts was determined by Bradford assay (Biorad). Proteins were resolved by 8 % acrylamide gel electrophoresis and transferred to a reinforced PVDF membrane (Amersham) or nitrocellulose (BA-S 83, Schleicher and Schuell, Keene, NH, USA). The membranes were blocked with 5 % non-fat dry milk in PBS 0.1 % Tween 20 and incubated with mouse anti-Per2 (1:500), rabbit anti-pS662PER2 (1:500), anti-fibrillarin (1:1,000, ab4566 Abcam) and anti-actin (1:10,000, Sigma) followed by incubation with the following secondary antibodies: goat anti-mouse and goat anti-rabbit (1:10,000), coupled with horseradish peroxidase, detected by enhanced chemiluminescence detection (Amersham, Arlington Heights, IL, USA).

Densitometric analysis was performed using the Quantity One Program (Bio-Rad Headquarters, Hercules, CA, USA). Briefly, the signal intensity for each band was calculated and the background subtracted from experimental values. The resulting values were then normalized and expressed as fold increase with respect to the control and mean values ± SEM.

Gene expression studies

Total RNA from ActD-treated and control HaCaT cells was collected with TRIzol (Invitrogen, Carlsbad, CA, USA) every 4 h for 36 consecutive h and purified according to manufacturer's instructions.

The total RNA concentration was quantified spectrophotometrically using NanoDrop (Thermo Scientific), and samples were stored at −80 °C. One microgram of total RNA was transcribed to cDNA with the iScript cDNA synthesis kit (Bio-Rad) according to the manufacturer's instructions. Real-time PCR was performed using the iCycler Real-Time Detection System (iQ5 Bio-Rad) with optimized PCR conditions. The reaction was carried out in 96-well plates using iQ SYBR Green Supermix (Bio-Rad) adding forward and reverse primers for each gene and 40 ng of template cDNA into a final

reaction volume of 15 µl. The thermal cycling program was performed as follows: an initial denaturation step at 95 °C for 3 min, followed by 45 cycles at 95 °C for 10 s and 60 °C for 30 s. Relative gene expression was assessed normalizing the cycle threshold (Ct) of each gene to ribosomal 18S RNA and expressing the data as ΔCt. Per2 versus Per2S relative expression levels were estimated as previously reported [40] using b/b′ and c/c′ primers upon verification of their similar amplification efficiency assayed as specified in the User Bulletin #2 (Applied Biosystems). New 45S rRNA synthesis was monitored by qRT-PCR as previously described [41] and data expressed as fold changes of 45S expression at the specific time point versus control (T0). Primer sequences are provided in Supplementary Table S1.

Flow cytometry analysis

ActD-treated HaCaT cells were seeded into 6-cm Petri dishes until subconfluence was reached. Soon after treatment and every 4 h for 36 h, cells were detached with trypsin (Euroclone), resuspended in 70 % ethanol in PBS and stored at 4 °C overnight. Cells were washed with PBS, resuspended in propidium iodide (PI) staining solution (50 µg/ml) and RNAse A (100 Kunitz/ml) (MiltenyiBiotec GmbH, Bergisch Gladbach, Germany), and incubated in the dark for 40 min at room temperature. At least 20,000 cells for each culture were collected and analyzed with the MACSQuant® Analyzer cytometer (MiltenyiBiotec GmbH). Cell cycle distribution was calculated with MACSQuantify® software (MiltenyiBiotec GmbH).

Transmission electron microscopy

HaCaT cells, cultured until subconfluence was reached, were treated or not with ActD (0.01 µg/ml) for 1 h as above, washed three times in PBS and fixed with 2 % glutaraldehyde in PBS for 2 h at 4 °C. Samples were post fixed with 1 % osmium tetroxide in veronal acetate buffer (pH 7.4) for 1 h at 25 °C, stained with uranyl acetate (5 mg/ml) for 1 h at 25 °C, dehydrated in acetone and embedded in Epon 812 (EMbed 812, Electron Microscopy Science, Hatfield, PA, USA). Ultra-thin sections were examined unstained or post stained with uranyl acetate and lead hydroxide under a Morgagni 268D transmission electron microscope (FEI, Hillsboro, OR, USA) equipped with a Mega View II charge-coupled device camera [Soft Imaging System (SIS) GmbH, Munster, Germany) and analyzed with AnalySIS software (SIS).

Statistical analysis

All experiments were repeated independently at least three times. All data are expressed as mean ± SEM. Significance of time series was established using one-way ANOVA on detrended gene expression as described before [35]. The p values <0.05 were considered statistically significant and indicative that the series was dependent by the time. Fitting of gene expression data to a cosine wave was verified with CircWave software (http://www.euclock.org/shareware/CircWave%20V1.4.zip) and considered significant for R^2 values >0.6. To estimate Per2 $t_{1/2}$ versus Per2S $t_{1/2}$, the percentage of mRNA levels (normalized to 18S) at each time point of 5 µg/ml ActD treatment was calculated. Normalized mRNA levels in the absence of ActD ($t = 0$) were considered as 100 %. The half-life of each isoform was obtained by first decay non-linear regression analysis using the equation $t_{1/2} = \ln 2/k$ as previously reported [42]. All the statistical analyses were performed using Graphpad Prism v 5.0 software. Nucleolar area quantification was estimated using ImageJ software [43].

Results

Comparison between Per2 and Per2S cDNA and protein sequences

The analysis of the Per2S versus Per2 coding sequence (cds) revealed that Per2S is 1,215 base pairs (bp) long, corresponding to a protein of 404 amino acids (AA), while Per2 cds is much longer, 3,767 bp, codifying for a protein of 1,255 AA. Sequence comparison displayed that nucleotides from 1–1,046 to 1,155 to 1,215 were present in both Per2 and Per2S. The regions spanning nucleotides 1,047–1,154 and 1,216–3,767 were present only in Per2 cds (Fig. 1a).

At a protein level PER2 and PER2S had complete homology in the N-terminal region from 1 to 348 AA. Both PER2 and PER2S shared the region from 181 to 284 AA containing the Per-Arnt-Sim domain A (PAS A). The second PAS domain of PER2 (PAS B, from 321 to 348 AA) was truncated in PER2S at position 348 where the homology between PER2 and PER2S was lost (Fig. 1b). Interestingly, the co-activator-like protein/protein interaction motif (LXXLL, 308–313 AA) of PER2, which mediates the binding to several nuclear receptors including REV-ERBα and PPARα [44], was conserved in PER2S (Fig. 1b). Computational analysis using BLAST [45] and SMART [46], web-based bio-informatic tools, revealed that the PER2S C-terminal region had no sequence homology or conserved motif with any annotated proteins in both databases. PER2S had neither nuclear (NLS) nor nucleolar import signals (NoLS) as predicted using the NucPred [47] and NoD [48] web-based tools, respectively.

In summary, our computational analysis indicates that the absence in Per2S of nucleotides from 1,047 to 1,154

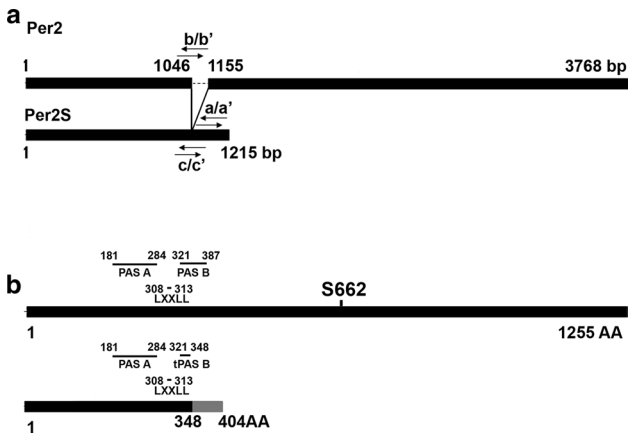

Fig. 1 Per2 and Per2S cDNA and protein coding sequences. **a** Per2 and Per2S nucleotide cds comparison: Per2 and Per2S share nucleotides from 1–1,046 to 1,155–1,215. The regions between nucleotides 1,047 and 1,154 and from 1,215 to 3,767 are present only in Per2 cds. Primers specifically designed to recognize both Per2 splicing variants (a/a′), only Per2 (b/b′) or only Per2S (c/c′) are shown. **b** Per2 and Per2S protein sequence comparison: Per2 and Per2S have complete homology in the N-terminal region from 1 to 348 AA, sharing AA from 181 to 284, which contain the Per-Arnt-Sim domain A (PAS A). The second PAS domain of Per2 (PAS B, from 321 to 348 AA) is truncated in Per2S (tPASB) at position 348 where the homology between Per2 and Per2S is lost. The co-activator-like protein/protein interaction motif (LXXLL) is present on both proteins (from 308 to 313 AA). Per2S cDNA and protein diagrams in **a** and **b** are scaled relatively to Per2 cDNA or protein sequences length

was responsible for the loss of Per2/Per2S protein homology at the C-terminal. PER2S displays conserved protein/protein interaction motifs in the N-terminal region; it is not conserved at the C-terminal and does not contain any NLS or NoLS.

Expression and circadian oscillation of Per2S isoform in human keratinocytes

In order to assess whether Per2S mRNA was effectively present in human cells, its expression was evaluated by qRT-PCR in asynchronous cultures of HaCaT cells.

Three different sets of primers were designed based on Per2 and Per2S cds alignment: the couple of primers a/a' amplifying a region in common to both Per2 and Per2S, b/b′ recognizing a region specific only to Per2 and c/c′ recognizing a region specific only to Per2S (Fig. 1a). Each couple of primers (a/a′, b/b′ and c/c′) gave rise to a specific melting curve as assessed by qRT-PCR, this demonstrating that both Per2 isoforms were expressed in HaCaT cells (Fig. 2a). The presence of Per2S transcript in asynchronous cultures of HaCaT cells prompted us to investigate whether this second splicing variant could display circadian oscillation upon clock synchronization. HaCaT cells can be entrained by the gold standard synchronizing agent Dex [35]. Serum-starved HaCaT cells were treated with 100 nM of Dex for 1 h and then released in the absence of serum for 36 consecutive h. Total RNA was sampled every 4 h and assayed by qRT-PCR using primers specific for Bmal1, Rev-Erbα, Per2 and Per2S. HaCaT cells left untreated during the entire time course were used as control for endogenous circadian oscillation of the set of genes selected for the analysis. As expected, Dex treatment induced significant circadian oscillation of the core clock gene Bmal1 (Fig. 2b), which was anti-phasic with its repressors Rev-Erbα (Fig. 2c) and Per2 (Fig. 2d) genes [49]. Importantly, Per2S gene also displayed a periodic oscillation that was anti-phasic to Bmal1 (Fig. 2e). Control HaCaT cells did not show significant oscillation of any of the genes considered in our analysis (Fig. 2b–e, left panels). All the experiments were repeated at least three times, and circadian oscillation was statistically verified by one-way ANOVA and fitting expression data to a cosine wave [50].

Taken together, our results indicate for the first time that the Per2S splicing variant is expressed in HaCaT cells and that it oscillates in response to the molecular clock synchronization induced by Dex treatment.

PER2S protein isoform is abundantly expressed and localizes in the nucleolus of human keratinocytes

In order to assess the expression and intracellular localization of PER2S protein, biochemical assays and immunofluorescence analysis were performed in asynchronous HaCaT cells. WB analysis performed on whole-cell lysates using an antibody raised against the recombinant human PER2 protein (abRc) constantly revealed the presence of two main bands: the first band at the expected size of ~140 kDa and the second at the lower molecular weight of ~55 kDa, which was comparable to the expected size for Per2S protein (~45 kDa) (Fig. 3a). Surprisingly, the lower and non-canonical band usually displayed a stronger signal compared to the normal PER2 band at ~140 kDa, which was not visible upon short exposure of our membranes (Supplementary Fig. S1). This suggested that the abRc antibody could recognize an epitope shared between PER2 and PER2S protein. In order to verify this hypothesis, the same whole-cell lysates were analyzed by WB using an antibody raised against the phospho-serine 662 (abS662), the AA residue that when mutated is responsible for the familiar advanced sleep phase syndrome [21] and that should be completely absent in PER2S protein (Fig. 1b). As expected, the abS662 antibody detected only PER2 protein as demonstrated by the presence of a single band at ~140 kDa (Fig. 3b). Therefore, we concluded that while the abRc antibody was able to recognize both PER2 and PER2S isoforms, the abpS662 was specific only for PER2. Moreover, since the ~55 kDa band was always

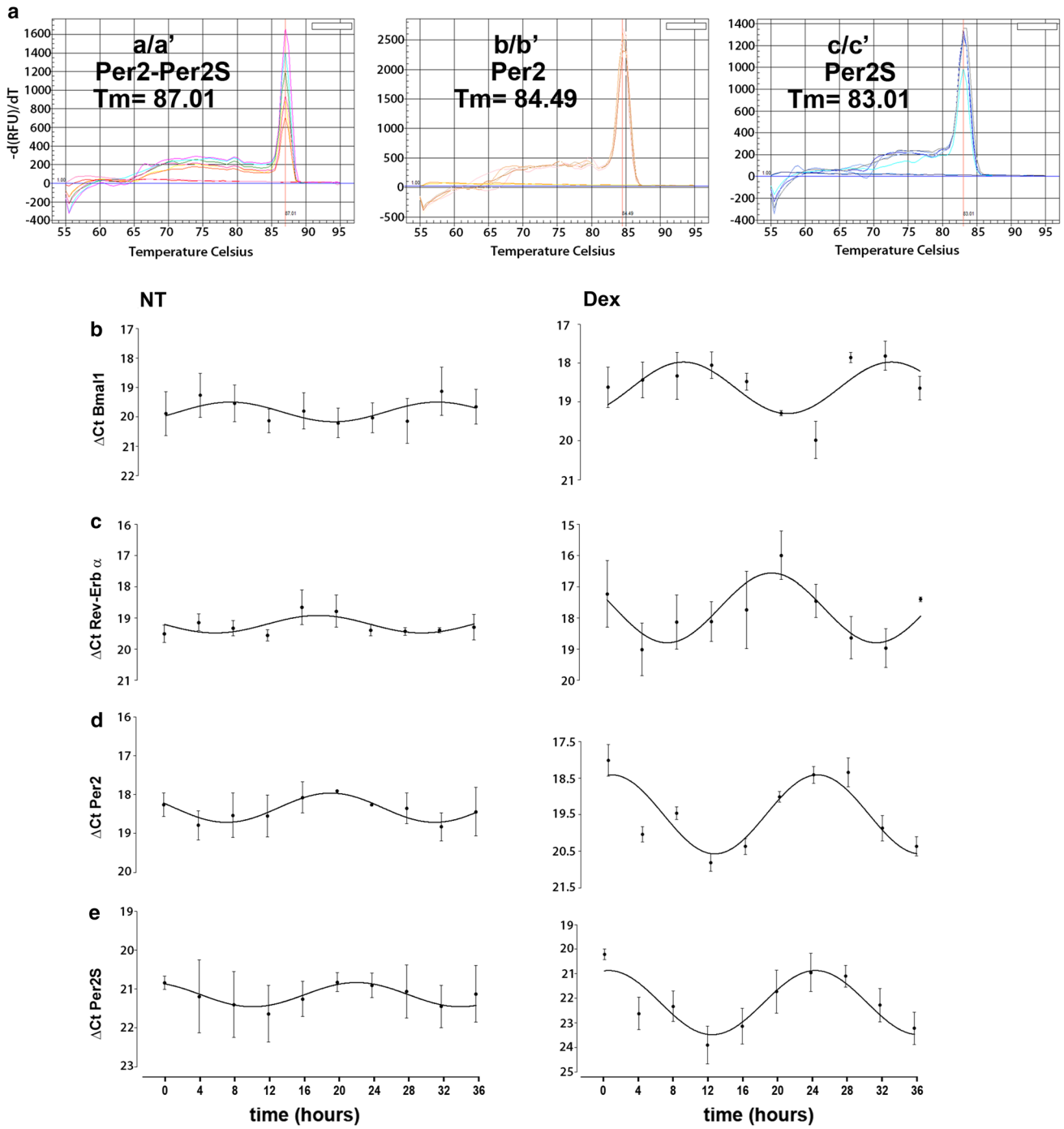

Fig. 2 Expression and circadian synchronization of the Per2S splicing variant. **a** Specific primers for both isoforms (a/a′), only for Per2 (b/b′) and only for Per2S (c/c′) were designed and used to amplify cDNA from asynchronous HaCaT cells. Melting curves for a/a′, b/b′ and c/c′ and their relative melting temperatures are shown. Quantitative RT-PCR showing significant circadian oscillation of Bmal1 (**b**), Rev-Erbα (**c**), Per2 (**d**) and Per2S (**e**) in Dex-treated cells (*right panel*) compared to untreated HaCaT cells (*left panel*). Data are expressed as the mean of ΔCt ± SEM calculated from the Ct value of each gene minus the corresponding 18S Ct ($n = 3$); *$p < 0.05$, one-way ANOVA; #cosinor analysis: $R^2 > 0.6$, data from all time points are presented

significantly more intense than the band at ~140 kDa, we concluded that PER2S was either more abundant or abRc recognized this isoform more efficiently. To address this issue, we compared Per2 versus Per2S basal expression and decay ($t_{1/2}$). The expression levels of Per2 versus Per2S were estimated upon experimental verification that both b/b′ and c/c′ primers have the same amplification efficiency (Supplementary Fig. S2a) as already reported elsewhere

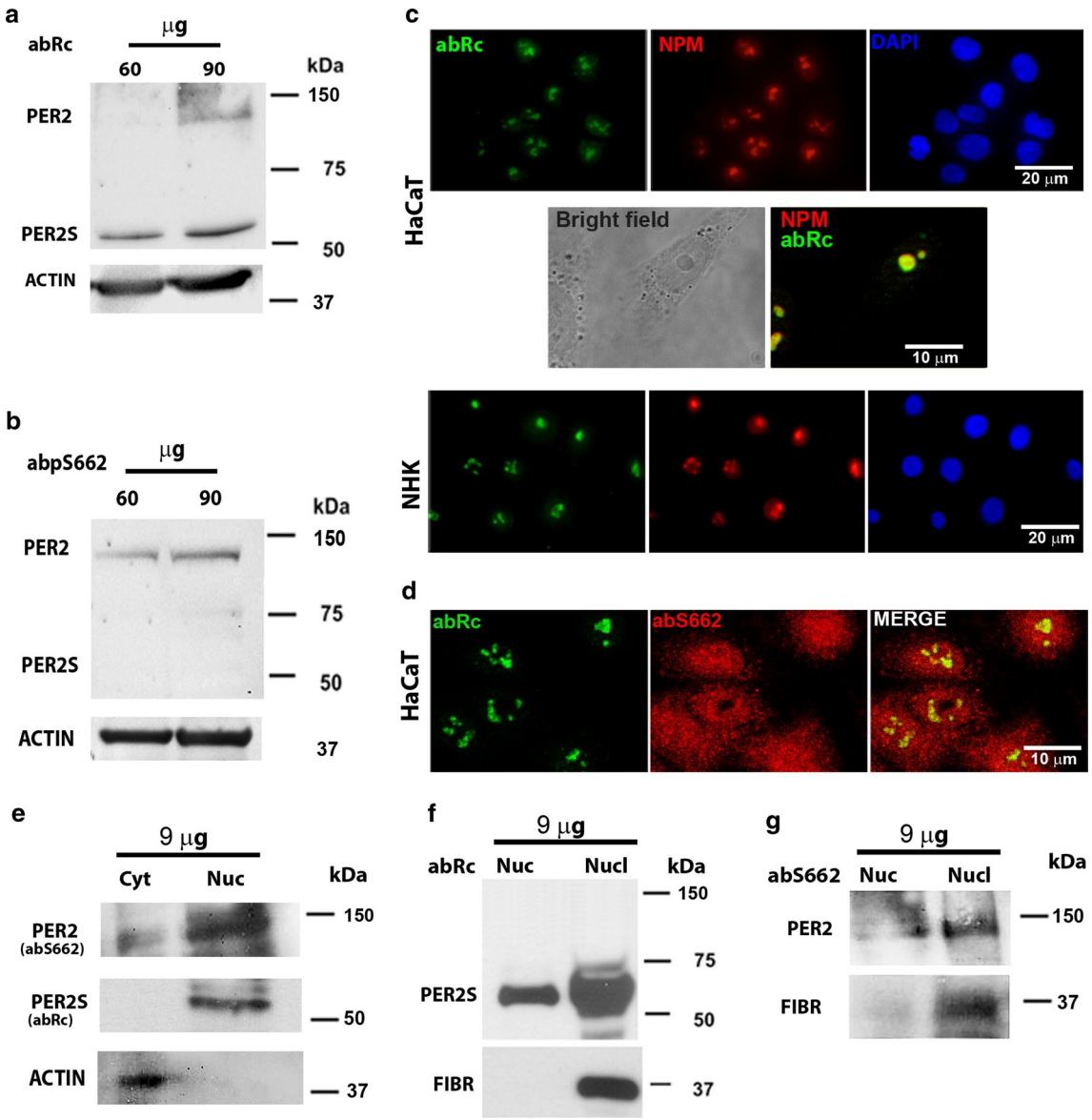

Fig. 3 PER2S is enriched in the nucleolus of human keratinocytes. **a** Western blot (WB) analysis loading 60 and 90 μg of whole protein extracts of asynchronous HaCaT cells showing PER2 isoforms. The abRc antibody detects two bands: one at ~55 kDa and one at ~140 kDa. The higher band is visible only loading 90 μg of protein extract and upon long exposure of the membrane. **b** The abS662 antibody detects only the higher band at ~140 kDa. **c** Immunofluorescence analysis showing colocalization of PER2 isoforms (abRc, *green*) and nucleophosmin (NPM, *red*) in asynchronous HaCaT cells (*upper panel*) and in NHKs (*lower panel*). Cell nuclei were visualized by DAPI (*blue*); *scale bar* 20 μm. Bright field image highlighting the colocalization of abRc and NPM in the nucleolus of HaCaT cells (*middle panel*); *scale bar* 10 μm. **d** Confocal image of asynchronous HaCaT cells showing colocalization of the PER2 nuclear signal (abS662, *red*) and nucleolar signal (abRc, *green*) and merge; *scale bar* 10 μm. **e** WB analysis of proteins isolated from cytoplasmic (Cyt) and nuclear (Nuc) fractions showing PER2 (abS662) in the cytoplasmic and nuclear fractions, but PER2S only in the nuclear fraction; β-actin (ACTIN) was used as a marker of cytoplasm. **f** WB analysis using abRc antibody showing PER2S in the nuclear (Nuc) and nucleolar (Nucl) fractions. **g** The same experiment was repeated using abS662 antibody to detect PER2 protein. Fibrillarin (FIBR) was used as a specific nucleolar marker of the nucleolus

[40]. Our results indicated that Per2 was significantly more expressed than Per2S in asynchronous HaCaT cells (ΔCt Per2 = 18.42 ± 0.54 versus ΔCt Per2S = 21.00 ± 0.75, Student's t test $p < 0.05$). To estimate Per2 versus Per2S $t_{1/2}$, cell transcription was completely blocked using 5 μg/ml of ActD [38], and Per2 versus Per2S expression levels were measured at 0, 1, 4 and 8 h of the treatment. No significant differences of Per2 versus Per2S $t_{1/2}$ were observed (Supplementary Fig. S2b).

In order to exclude the possibility that the ~55 kDa could represent a degradation product of PER2, the potential cleavage sites of a large panel of proteases were predicted

using two different web-based tools: PeptideCutter [51] and PROSPER [52]. Most of the analyzed proteases displayed multiple putative cleavage sites. Only calpain-1, thrombin and caspase 1 were predicted to recognize a single residue resulting in one single cut. However, the molecular weights of the predicted fragments were never consistent with the ~55 kDa band (Supplementary Table S2). Taken together, these results indicate that abRc recognizes the ~55 kDa more efficiently than the ~140 kDa band; therefore, the relative intensity of the two bands could not be strictly associated with the different amounts of the two isoforms.

Since a detailed analysis of the PER2 intracellular distribution in human keratinocytes is still lacking and the possible differential localization of the two PER2 isoforms (PER2 and PER2S) has never been addressed, we took advantage of the different affinities of abRc and abpS662 antibodies to study PER2 and PER2S intracellular localization in HaCaT cells. Surprisingly and very interestingly, the immunofluorescence analysis using the abRc antibody revealed that the signal was prevalently localized in the nucleus with a peculiar strong concentration in the nucleolar compartment as confirmed by colocalization with the nucleolar marker nucleophosmin (NPM) [53] and visualization of nucleoli using the bright field (Fig. 3c, upper and middle panels). This peculiar localization was also observed in NHKs, demonstrating that it is a general phenomenon occurring also on primary cultured cells (Fig. 3c, lower panel). Confocal analysis revealed that the abS662 antibody signal was diffuse and mainly distributed in the nucleus and partially in the cell cytoplasm (Fig. 3d). Importantly, a small amount of the nuclear abS662 staining colocalized with the abRc signal in the nucleolus.

In order to confirm these observations, cytoplasmic and nuclear fractions were isolated from HaCaT cells and then analyzed by WB using both abRc and abS662 antibodies. Equal amounts of proteins were loaded for each cellular fraction in order to precisely establish the relative distribution of PER2 and PER2S isoforms in the different cellular compartments. WB analysis confirmed our immunostaining results: abS662 antibody detected a band at ~140 kDa, corresponding to PER2 in both the cytoplasmic and nuclear fractions, whereas the abRc antibody revealed a single band at ~55 kDa, corresponding to PER2S, only in the nucleus (Fig. 3e). In order to confirm the presence of PER2 and PER2S in the nucleolar compartment, nuclear and nucleolar fractions were isolated using a specific protocol [39], and proteins were analyzed by WB. Interestingly, PER2S was present in the nuclear and in the nucleolar fraction as confirmed by the specific nucleolar marker fibrillarin (Fig. 3f). Similarly, PER2 reactivity was also found in both the nuclear and nucleolar fractions (Fig. 3g).

Finally, since PER2 is known to interact with other components of the core clock machinery, in order to assess whether other components of the cellular clock could localize in the nucleolus of HaCaT cells, the intracellular distribution of BMAL1, CLOCK and CRY2 proteins was assessed by immunofluorescence coupled to the detection of the nucleoli using the bright field (Supplementary Fig. S3a): as expected BMAL1 and CLOCK proteins were mainly expressed in the nucleus [54, 55], whereas CRY2 was nuclear and cytoplasmic [56]. Careful analysis through confocal serial sections crossing the nucleus revealed that none of them displayed clear nucleolar localization (Supplementary Fig. S3b).

Taken together, these results show that the PER2S isoform is enriched in the nucleolus of human keratinocytes.

Actinomycin D induces reversible changes in the nucleolar structure and Per2 localization

By using a short pulse (1 h) of 0.01 μg/ml ActD followed by a chase in full medium, we set up the conditions to reach a minimum level of polymerase I impairment, this resulting in a transient and reversible nucleolar disruption. Nucleolar integrity and PER2S isoform localization and shuttling were investigated under these experimental conditions.

The ultrastructural analysis of untreated (NT) and ActD short-pulsed HaCaT cells was performed soon after drug removal (T0) (Fig. 4a). NT cells showed a conventional distribution of all nucleolar substances with the granular component (GC), which represents the main body of the nucleolus, and the nucleolonema [dense fibrillar component (DFC)] arranged around patches of low electron dense material (fibrillar centers), (Fig. 4a, NT: first and second panel). In contrast, several nucleolar changes were observed in T0 cells, such as the coalescence of DFCs to form compact round aggregates (Fig. 4a, T0: first and second panel), the progressive sorting out of nucleolar components into larger aggregates (Fig. 4a, T0: second panel) and the reduction of overall nucleolar size (Fig. 4a, T0: third panel). These nucleolar alterations are consistent with what has been reported previously in similar experiments [57].

Next, nucleolar areas were manually measured using the image tool analysis software ImageJ [43], and mean areas were calculated from at least 200 measures for each time point. Our analysis showed that the nucleolar area decreased significantly at T0 and returned gradually to the original size (NT) at T6 and T24 (Fig. 4b).

The effect of ActD on PER2S localization was evaluated by immunofluorescence using abRc antibody in NT, T0, T6 and T24 samples. PER2S de-localized predominantly to the nucleoplasm and cytoplasm soon after ActD treatment (Fig. 4c, T0). Partial and complete PER2S re-localization within the nucleolus was observed at T6 and T24, respectively. NPM was used to track nucleolar fate under the same experimental conditions [41, 53].

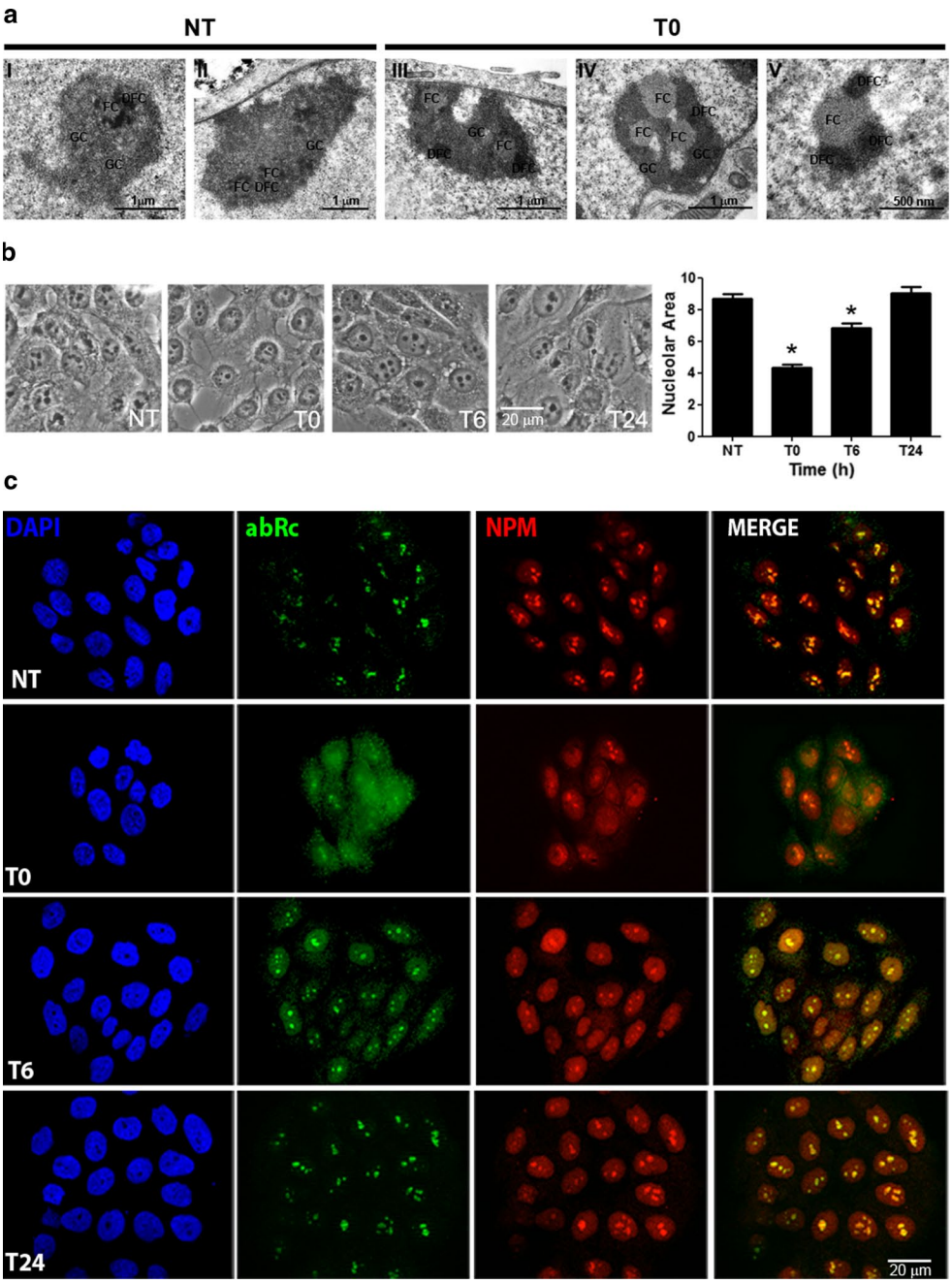

Fig. 4 Actinomycin D induces reversible nucleolar structural modifications and PER2 de-localization from the nucleolus. **a** Transmission electron microscopy picture showing nucleolar changes in untreated (NT) HaCaT cells or treated with 0.01 µg/ml of ActD for 1 h (T0). *I*, *II*: nucleolus of untreated HaCaT cells; *III–V*: segregation and coalescence of nucleolar components in ActD-treated HaCaT cells. *Scale bars I–IV* 1 µm, *V* 0.5 µm. *GC* granular component, *DFC* dense fibrillar component (or nucleolonema), *FC* fibrillar center. **b** Phase contrast microscopy pictures of HaCaT cells treated as in **a** and then released in DMEM in the presence of FBS 10 % for 6 (T6) and 24 h (T24). Quantification of the nucleolar area is reported. Not <200 cells for each time point were considered in the statistical analysis. $*p < 0.05$, one-way ANOVA followed by Newman-Keuls test. *Scale bar* 20 µm. **c** Immunofluorescence analysis showing reversible de-localization of abRc signal (*green*) and NPM (*red*) in NT, T0, T6 and T24 cells. The abRc signal is increased in the nucleus and cytoplasm soon after ActD treatment. Re-localization of the abRc signal within the nucleolus is observed partially at T6 and completely at T24. Cell nuclei are visualized by DAPI. *Scale bar* 20 µm

Finally, the effect of a short pulse of 0.01 µg/ml ActD on cell cycle and nucleolar function was assessed sampling HaCaT cells every 4 h for 36 consecutive h. Cytofluorimetric analysis showed that the cell cycle was not significantly influenced by this treatment, as the percentage of cells in G0/G1 did not vary over a period of time spanning 36 h (Supplementary Fig. S4a). Moreover, the short pulse of ActD did not block nucleolar function, since the amount of newly synthesized rRNA 45S did not significantly change over time. On the other hand, the 45S rRNA expression was significantly impaired when ActD was left in the medium for the duration of the experiment (Supplementary Fig. S4b).

In conclusion, our results show that a single ActD pulse is able to reversibly change the nucleolar structure leading to consequent PER2S de-localization from the nucleolus to the nucleoplasmic and cytoplasmic compartments and to its return to the original localization within 24 h after the treatment. In addition, reversible structural changes are not associated with an evident impairment of cell function as demonstrated by cell cycle analysis and 45S rRNA expression analysis.

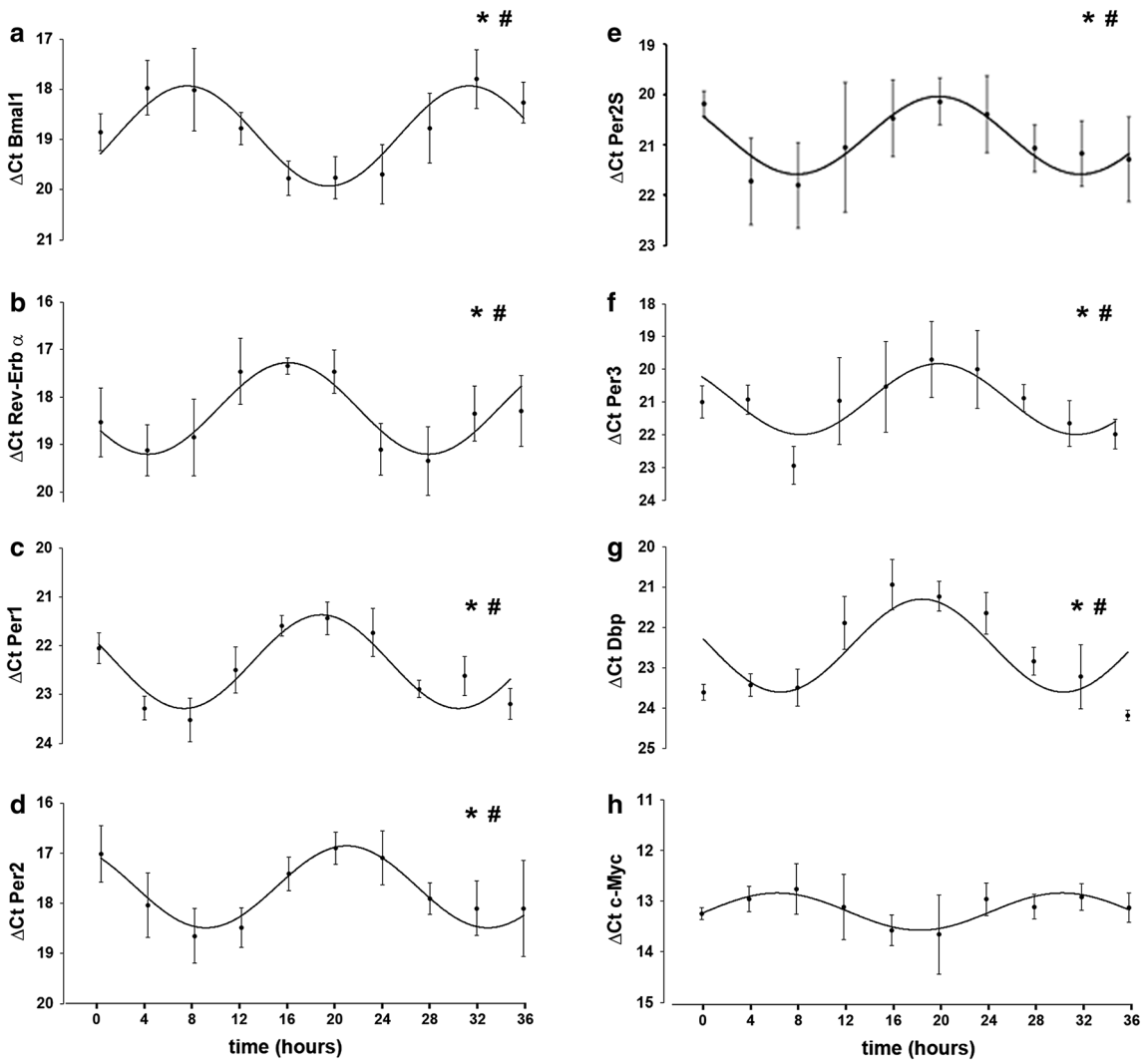

Fig. 5 Circadian synchronization of HaCaT cells in response to actinomycin D. Quantitative RT-PCR showing significant circadian oscillation of **a** Bmal1, **b** Rev-Erbα, **c** Per1, **d** Per2, **e** Per2S, **f** Per3 and **g** Dbp in ActD-treated cells. **h** The c-myc gene did not show any significant oscillation**. Data are expressed as the mean of $\Delta Ct \pm SEM$ calculated from the Ct value of each gene minus the corresponding 18S Ct ($n \geq 3$). *$p < 0.05$, one-way ANOVA; #cosinor analysis: $R^2 > 0.6$, data from all time points are presented

Circadian oscillation of clock genes in response to nucleolar stress

The nuclear/cytoplasmic shuttling of PER2 and other components of the core clock is necessary for proper cell entrainment. The reversible de-localization of PER2S in response to ActD treatment and the absence of a significant impairment of cellular functions prompted us to verify whether the ActD-induced nucleolar perturbation was able to circadianly synchronize the molecular clock. Gene expression analysis was performed on the total RNA sampled every 4 h for 36 consecutive h upon short ActD pulse. Cells left untreated (NT) were used as negative control for clock synchronization. ActD induced the significant anti-phasic and periodic oscillation of the core clock genes Bmal1, Rev-erbα and Per2 (Fig. 5a, b, d). Noteworthily, as already observed for Dex treatment, ActD was able to induce the periodic oscillation of the Per2S gene (Fig. 5e). Interestingly, also the other components of the Period family (Per1 and Per3; Fig. 5c, f) and the output gene Dbp (Fig. 5g) were circadianly synchronized under this experimental condition. Another clock-controlled gene, c-Myc, did not display any significant oscillation (Fig. 5h).

In conclusion, our results show for the first time that a transient perturbation of the nucleolar structure is sufficient to act as a powerful resetting stimulus, synchronizing both core clock genes (including PER2S) and the clock output gene Dbp.

Discussion

Our study provides the first evidence that Per2S, the second splicing variant of Per2, is expressed at both the mRNA and protein level in human keratinocytes, oscillating with a circadian period upon clock synchronization. Importantly, we show that PER2S preferentially localizes within the nucleolar compartment and that the transient perturbation of the nucleolar structure is associated with PER2S de-localization. These results suggest that nucleolar perturbation acts as a resetting stimulus inducing circadian oscillations of both the core clock genes and Dbp clock controlled gene. As a consequence, the nucleolus could have a direct role in the regulation of the circadian clock with PER2S as the main actor in such regulation. In line with this hypothesis, it is interesting to note that high temperature and ultraviolet rays have been shown to induce both changes in nucleolar structure and composition [53, 58–60] and circadian synchronization [30, 61].

Current models of the molecular clock functioning involve PER interaction with CRY proteins and subsequent translocation from the cytoplasm to the nucleus where they physically repress BMAL1/CLOCK heterodimers. PER2 nuclear translocation is necessary both for the circadian clock resetting [11, 12] and for the regulation of the period length [62, 63]. The demonstration that PER2S is enriched within the nucleolus implicates the need for an important revision of the current models of the molecular pathways regulating circadian synchronization.

It is now well documented that only 30 % of the nucleolar proteins directly participate in ribosome biogenesis. Other nucleolar proteins have functions implicated in the cell cycle, DNA repair, cell senescence and cellular stress response [39, 64]. Interestingly, some of the nucleolar-regulated processes are also controlled by the circadian systems [13, 15, 58, 65]. Intriguingly, the nucleolus has been shown to play a central role in the regulation of the p53 pathway [36, 41, 53]. When the nucleolar structure is disrupted in response to stress, the tumour suppressor ARF and ribosomal components RPL11, RPL5, RPL23 and RPS7 are released from the nucleolus into the nucleoplasm where they associate with MDM2, inhibiting its E3 ubiquitin ligase activity toward the p53 onco-suppressor and thus promoting p53 stabilization and activation [66]. Therefore, under stress conditions PER2S de-localization from the nucleolus could be important for transferring information about the physiological status of the nucleolus to the circadian system. PER2S could act as a sensor of time within the nucleolus transmitting the circadian clock information to the nucleolar components. This could favor a rapid nucleolar response to circadian clock changes induced by external stimuli. Indeed, PER2 protein has been implicated in the coupling of the circadian clock to metabolism by modulating the transcriptional activity of numerous nuclear receptors including REV-ERBα, PPARα, PPARγ and HNF4α [44, 67]. This regulatory activity of PER2 has been shown to be mediated by its ability to establish protein/protein interaction through its PAS domains and the LXXLL, which are remarkably conserved also at the N-termini of PER2S.

In summary, the present work demonstrates the existence of a cross talk between the nucleolus and the circadian clock, which is possibly mediated by the activity of PER2S. These important issues are currently under investigation and will be the object of future studies. We are confident that our work will strongly contribute to gaining new important insights regarding the mechanisms governing the circadian clock and nucleolar function, which, when deregulated, have an important role in cancer development.

Acknowledgments This work was partially supported by grants from the Italian Space Agency (ASI, I/003/11/0), MIUR and the Associazione Italiana per la Ricerca sul Cancro (AIRC, IG 10272), Italy.

Conflict of interest The authors declare no conflict of interest.

References

1. Geyfman M, Andersen B (2009) How the skin can tell time. J Invest Dermatol 129(5):1063–1066. doi:10.1038/jid.2008.384
2. Schibler U (2006) Circadian time keeping: the daily ups and downs of genes, cells, and organisms. Prog Brain Res 153:271–282. doi:10.1016/S0079-6123(06)53016-X
3. Guillaumond F, Dardente H, Giguere V, Cermakian N (2005) Differential control of Bmal1 circadian transcription by REV-ERB and ROR nuclear receptors. J Biol Rhythm 20(5):391–403. doi:10.1177/0748730405277232
4. Kojima S, Shingle DL, Green CB (2011) Post-transcriptional control of circadian rhythms. J Cell Sci 124(Pt 3):311–320. doi:10.1242/jcs.065771
5. Panda S, Antoch MP, Miller BH, Su AI, Schook AB, Straume M, Schultz PG, Kay SA, Takahashi JS, Hogenesch JB (2002) Coordinated transcription of key pathways in the mouse by the circadian clock. Cell 109(3):307–320
6. Reddy AB, Karp NA, Maywood ES, Sage EA, Deery M, O'Neill JS, Wong GK, Chesham J, Odell M, Lilley KS, Kyriacou CP, Hastings MH (2006) Circadian orchestration of the hepatic proteome. Curr Biol 16(11):1107–1115. doi:10.1016/j.cub.2006.04.026
7. Storch KF, Lipan O, Leykin I, Viswanathan N, Davis FC, Wong WH, Weitz CJ (2002) Extensive and divergent circadian gene expression in liver and heart. Nature 417(6884):78–83. doi:10.1038/nature744
8. Golombek DA, Casiraghi L, Agostino PV, Paladino N, Duhart J, Plano SA, Chiesa JJ (2013) The times are changing: effects of circadian desynchronization on physiology and disease. J Physiol Paris. doi:10.1016/j.jphysparis.2013.03.007
9. Lee S, Donehower LA, Herron AJ, Moore DD, Fu L (2010) Disrupting circadian homeostasis of sympathetic signaling promotes tumor development in mice. PLoS One 5(6):e10995. doi:10.1371/journal.pone.0010995
10. Eckel-Mahan K, Sassone-Corsi P (2013) Metabolism and the circadian clock converge. Physiol Rev 93(1):107–135. doi:10.1152/physrev.0 0016.2012

11. Albrecht U, Zheng B, Larkin D, Sun ZS, Lee CC (2001) MPer1 and mper2 are essential for normal resetting of the circadian clock. J Biol Rhythms 16(2):100–104
12. Spoelstra K, Albrecht U, van der Horst GT, Brauer V, Daan S (2004) Phase responses to light pulses in mice lacking functional per or cry genes. J Biol Rhythm 19(6):518–529. doi:10.1177/0748730404268122
13. Fu L, Pelicano H, Liu J, Huang P, Lee C (2002) The circadian gene Period2 plays an important role in tumor suppression and DNA damage response in vivo. Cell 111(1):41–50
14. Gery S, Gombart AF, Yi WS, Koeffler C, Hofmann WK, Koeffler HP (2005) Transcription profiling of C/EBP targets identifies Per2 as a gene implicated in myeloid leukemia. Blood 106(8):2827–2836. doi:10.1182/blood-2005-01-0358
15. Hua H, Wang Y, Wan C, Liu Y, Zhu B, Yang C, Wang X, Wang Z, Cornelissen-Guillaume G, Halberg F (2006) Circadian gene mPer2 overexpression induces cancer cell apoptosis. Cancer Sci 97(7):589–596. doi:10.1111/j.1349-7006.2006.00225.x
16. Miyazaki K, Wakabayashi M, Hara Y, Ishida N (2010) Tumor growth suppression in vivo by overexpression of the circadian component, PER2. Genes Cells 15(4):351–358. doi:10.1111/j.1365-2443.2010.01384.x
17. Oda A, Katayose Y, Yabuuchi S, Yamamoto K, Mizuma M, Shirasou S, Onogawa T, Ohtsuka H, Yoshida H, Hayashi H, Rikiyama T, Kim H, Choe Y, Kim K, Son H, Motoi F, Egawa S, Unno M (2009) Clock gene mouse period2 overexpression inhibits growth of human pancreatic cancer cells and has synergistic effect with cisplatin. Anticancer Res 29(4):1201–1209
18. Winter SL, Bosnoyan-Collins L, Pinnaduwage D, Andrulis IL (2007) Expression of the circadian clock genes Per1 and Per2 in sporadic and familial breast tumors. Neoplasia 9(10):797–800
19. Gallego M, Kang H, Virshup DM (2006) Protein phosphatase 1 regulates the stability of the circadian protein PER2. Biochem J 399(1):169–175. doi:10.1042/BJ20060678
20. Gu X, Xing L, Shi G, Liu Z, Wang X, Qu Z, Wu X, Dong Z, Gao X, Liu G, Yang L, Xu Y (2012) The circadian mutation PER2(S662G) is linked to cell cycle progression and tumorigenesis. Cell Death Differ 19(3):397–405. doi:10.1038/cdd.2011.103
21. Toh KL, Jones CR, He Y, Eide EJ, Hinz WA, Virshup DM, Ptacek LJ, Fu YH (2001) An hPer2 phosphorylation site mutation in familial advanced sleep phase syndrome. Science 291(5506):1040–1043
22. Asher G, Gatfield D, Stratmann M, Reinke H, Dibner C, Kreppel F, Mostoslavsky R, Alt FW, Schibler U (2008) SIRT1 regulates circadian clock gene expression through PER2 deacetylation. Cell 134(2):317–328. doi:10.1016/j.cell.2008.06.050
23. Ohsaki K, Oishi K, Kozono Y, Nakayama K, Nakayama KI, Ishida N (2008) The role of {beta}-TrCP1 and {beta}-TrCP2 in circadian rhythm generation by mediating degradation of clock protein PER2. J Biochem 144(5):609–618. doi:10.1093/jb/mvn112
24. Miki T, Xu Z, Chen-Goodspeed M, Liu M, Van Oort-Jansen A, Rea MA, Zhao Z, Lee CC, Chang KS (2012) PML regulates PER2 nuclear localization and circadian function. EMBO J 31(6):1427–1439. doi:10.1038/emboj.2012.1
25. Miyazaki K, Mesaki M, Ishida N (2001) Nuclear entry mechanism of rat PER2 (rPER2): role of rPER2 in nuclear localization of CRY protein. Mol Cell Biol 21(19):6651–6659
26. Yagita K, Yamaguchi S, Tamanini F, van Der Horst GT, Hoeijmakers JH, Yasui A, Loros JJ, Dunlap JC, Okamura H (2000) Dimerization and nuclear entry of mPER proteins in mammalian cells. Genes Dev 14(11):1353–1363
27. Tamanini F, Yagita K, Okamura H, van der Horst GT (2005) Nucleocytoplasmic shuttling of clock proteins. Methods Enzymol 393:418–435. doi:10.1016/S0076-6879(05)93020-6
28. Koyanagi S, Hamdan AM, Horiguchi M, Kusunose N, Okamoto A, Matsunaga N, Ohdo S (2011) cAMP-response element (CRE)-mediated transcription by activating transcription factor-4 (ATF4) is essential for circadian expression of the Period2 gene. J Biol Chem 286(37):32416–32423. doi:10.1074/jbc.M111.258970
29. McDearmon EL, Patel KN, Ko CH, Walisser JA, Schook AC, Chong JL, Wilsbacher LD, Song EJ, Hong HK, Bradfield CA, Takahashi JS (2006) Dissecting the functions of the mammalian clock protein BMAL1 by tissue-specific rescue in mice. Science 314(5803):1304–1308. doi:10.1126/science.1132430
30. Tamaru T, Hattori M, Honda K, Benjamin I, Ozawa T, Takamatsu K (2011) Synchronization of circadian Per2 rhythms and HSF1–BMAL1:CLOCK interaction in mouse fibroblasts after short-term heat shock pulse. PLoS One 6(9):e24521. doi:10.1371/journal.pone.0024521
31. Travnickova-Bendova Z, Cermakian N, Reppert SM, Sassone-Corsi P (2002) Bimodal regulation of mPeriod promoters by CREB-dependent signaling and CLOCK/BMAL1 activity. Proc Natl Acad Sci USA 99(11):7728–7733. doi:10.1073/pnas.102075599
32. Ikeda M, Nomura M (1997) cDNA cloning and tissue-specific expression of a novel basic helix-loop-helix/PAS protein (BMAL1) and identification of alternatively spliced variants with alternative translation initiation site usage. Biochem Biophys Res Commun 233(1):258–264. doi:10.1006/bbrc 1997.6371
33. Garcia-Fernandez JM, Alvarez-Lopez C, Cernuda-Cernuda R (2007) Cytoplasmic localization of mPER1 clock protein isoforms in the mouse retina. Neurosci Lett 419(1):55–58. doi:10.1016/j.neulet.2007.03.054
34. Sandu C, Dumas M, Malan A, Sambakhe D, Marteau C, Nizard C, Schnebert S, Perrier E, Challet E, Pevet P, Felder-Schmittbuhl MP (2012) Human skin keratinocytes, melanocytes, and fibroblasts contain distinct circadian clock machineries. Cell Mol Life Sci 69(19):3329–3339. doi:10.1007/s00018-012-1026-1
35. Sporl F, Schellenberg K, Blatt T, Wenck H, Wittern KP, Schrader A, Kramer A (2011) A circadian clock in HaCaT keratinocytes. J Invest Dermatol 131(2):338–348. doi:10.1038/jid.2010.315
36. Kalita K, Makonchuk D, Gomes C, Zheng JJ, Hetman M (2008) Inhibition of nucleolar transcription as a trigger for neuronal apoptosis. J Neurochem 105(6):2286–2299. doi:10.1111/j.1471-4159.2008.05316.x
37. Boukamp P, Petrussevska RT, Breitkreutz D, Hornung J, Markham A, Fusenig NE (1988) Normal keratinization in a spontaneously immortalized aneuploid human keratinocyte cell line. J Cell Biol 106(3):761–771
38. Koyama M, Matsuzaki Y, Yogosawa S, Hitomi T, Kawanaka M, Sakai T (2007) ZD1839 induces p15INK4b and causes G1 arrest by inhibiting the mitogen-activated protein kinase/extracellular signal-regulated kinase pathway. Mol Cancer Ther 6(5):1579–1587. doi:10.1158/1535-7163.MCT-06-0814
39. Andersen JS, Lam YW, Leung AK, Ong SE, Lyon CE, Lamond AI, Mann M (2005) Nucleolar proteome dynamics. Nature 433(7021):77–83. doi:10.1038/nature03207
40. Nishimura M, Yaguti H, Yoshitsugu H, Naito S, Satoh T (2003) Tissue distribution of mRNA expression of human cytochrome P450 isoforms assessed by high-sensitivity real-time reverse transcription PCR. Yakugaku Zasshi 123(5):369–375
41. Avitabile D, Bailey B, Cottage CT, Sundararaman B, Joyo A, McGregor M, Gude N, Truffa S, Zarrabi A, Konstandin M, Khan M, Mohsin S, Volkers M, Toko H, Mason M, Cheng Z, Din S, Alvarez R Jr, Fischer K, Sussman MA (2011) Nucleolar stress is an early response to myocardial damage involving nucleolar proteins nucleostemin and nucleophosmin. Proc Natl Acad Sci USA 108(15):6145–6150. doi:10.1073/pnas.1017935108
42. Ysla RM, Wilson GM, Brewer G (2008) Chapter 3. Assays of adenylate uridylate-rich element-mediated mRNA

decay in cells. Methods Enzymol 449:47–71. doi:10.1016/S0076-6879(08)02403-8
43. Schneider CA, Rasband WS, Eliceiri KW (2012) NIH Image to ImageJ: 25 years of image analysis. Nat Methods 9(7):671–675
44. Schmutz I, Ripperger JA, Baeriswyl-Aebischer S, Albrecht U (2010) The mammalian clock component PERIOD2 coordinates circadian output by interaction with nuclear receptors. Genes Dev 24(4):345–357. doi:10.1101/gad.564110
45. Altschul SF, Gish W, Miller W, Myers EW, Lipman DJ (1990) Basic local alignment search tool. J Mol Biol 215(3):403–410. doi:10.1016/S0022-2836(05)80360-2
46. Schultz J, Copley RR, Doerks T, Ponting CP, Bork P (2000) SMART: a web-based tool for the study of genetically mobile domains. Nucleic Acids Res 28(1):231–234. doi:10.1093/nar/28.1.231
47. Brameier M, Krings A, MacCallum RM (2007) NucPred—predicting nuclear localization of proteins. Bioinformatics 23(9):1159–1160. doi:10.1093/bioinformatics/btm066
48. Scott MS, Troshin PV, Barton GJ (2011) NoD: a nucleolar localization sequence detector for eukaryotic and viral proteins. BMC Bioinforma 12:317. doi:10.1186/1471-2105-12-317
49. Shearman LP, Zylka MJ, Weaver DR, Kolakowski LF Jr, Reppert SM (1997) Two period homologs: circadian expression and photic regulation in the suprachiasmatic nuclei. Neuron 19(6):1261–1269
50. Sandu C, Dumas M, Malan A, Sambakhe D, Marteau C, Nizard C, Schnebert S, Perrier E, Challet E, Pevet P, Felder-Schmittbuhl MP (2012) Human skin keratinocytes, melanocytes, and fibroblasts contain distinct circadian clock machineries. Cell Mol Life Sci. doi:10.1007/s00018-012-1026-1
51. Gasteiger E, Hoogland C, Gattiker A, Duvaud S, Wilkins M, Appel R, Bairoch A (2005) Protein identification and analysis tools on the ExPASy server. In: Walker J (ed) The proteomics protocols handbook. Humana Press, New York, pp 571–607. doi:10.1385/1-59259-890-0:571
52. Song J, Tan H, Perry AJ, Akutsu T, Webb GI, Whisstock JC, Pike RN (2012) PROSPER: an integrated feature-based tool for predicting protease substrate cleavage sites. PLoS One 7(11):e50300. doi:10.1371/journal.pone.0050300
53. Rubbi CP, Milner J (2003) Disruption of the nucleolus mediates stabilization of p53 in response to DNA damage and other stresses. EMBO J 22(22):6068–6077. doi:10.1093/emboj/cdg579
54. Kwon I, Lee J, Chang SH, Jung NC, Lee BJ, Son GH, Kim K, Lee KH (2006) BMAL1 shuttling controls transactivation and degradation of the CLOCK/BMAL1 heterodimer. Mol Cell Biol 26(19):7318–7330. doi:10.1128/MCB.00337-06
55. Zanello SB, Jackson DM, Holick MF (2000) Expression of the circadian clock genes clock and period1 in human skin. J Invest Dermatol 115(4):757–760. doi:10.1046/j.1523-1747.2000.00121.x
56. Thompson CL, Bowes Rickman C, Shaw SJ, Ebright JN, Kelly U, Sancar A, Rickman DW (2003) Expression of the blue-light receptor cryptochrome in the human retina. Invest Ophthalmol Vis Sci 44(10):4515–4521
57. Schoefl GI (1964) The effect of actinomycin d on the fine structure of the nucleolus. J Ultrastruct Res 10:224–243
58. Razorenova OV (2012) Brain and muscle ARNT-like protein BMAL1 regulates ROS homeostasis and senescence: a possible link to hypoxia-inducible factor-mediated pathway. Cell Cycle 11(2):213–214. doi:10.4161/cc.11.2.18786
59. Al-Baker EA, Boyle J, Harry R, Kill IR (2004) A p53-independent pathway regulates nucleolar segregation and antigen translocation in response to DNA damage induced by UV irradiation. Exp Cell Res 292(1):179–186
60. Moore HM, Bai B, Boisvert FM, Latonen L, Rantanen V, Simpson JC, Pepperkok R, Lamond AI, Laiho M (2011) Quantitative proteomics and dynamic imaging of the nucleolus reveal distinct responses to UV and ionizing radiation. Mol Cell Proteomics 10(10):M111.009241. doi:10.1074/mcp.M111.009241
61. Kawara S, Mydlarski R, Mamelak AJ, Freed I, Wang B, Watanabe H, Shivji G, Tavadia SK, Suzuki H, Bjarnason GA, Jordan RC, Sauder DN (2002) Low-dose ultraviolet B rays alter the mRNA expression of the circadian clock genes in cultured human keratinocytes. J Invest Dermatol 119(6):1220–1223. doi:10.1046/j.1523-1747.2002.19619.x
62. Xu Y, Toh KL, Jones CR, Shin JY, Fu YH, Ptacek LJ (2007) Modeling of a human circadian mutation yields insights into clock regulation by PER2. Cell 128(1):59–70. doi:10.1016/j.cell.2006.11.043
63. Vanselow K, Vanselow JT, Westermark PO, Reischl S, Maier B, Korte T, Herrmann A, Herzel H, Schlosser A, Kramer A (2006) Differential effects of PER2 phosphorylation: molecular basis for the human familial advanced sleep phase syndrome (FASPS). Genes Dev 20(19):2660–2672. doi:10.1101/gad.397006
64. Boisvert FM, van Koningsbruggen S, Navascues J, Lamond AI (2007) The multifunctional nucleolus. Nat Rev Mol Cell Biol 8(7):574–585. doi:10.1038/nrm2184
65. Eckle T, Hartmann K, Bonney S, Reithel S, Mittelbronn M, Walker LA, Lowes BD, Han J, Borchers CH, Buttrick PM, Kominsky DJ, Colgan SP, Eltzschig HK (2012) Adora2b-elicited Per2 stabilization promotes a HIF-dependent metabolic switch crucial for myocardial adaptation to ischemia. Nat Med 18(5):774–782. doi:10.1038/nm.2728
66. Suzuki A, Kogo R, Kawahara K, Sasaki M, Nishio M, Maehama T, Sasaki T, Mimori K, Mori M (2012) A new PICTure of nucleolar stress. Cancer Sci 103(4):632–637. doi:10.1111/j.1349-7006.2012.02219.x
67. Ripperger JA, Schmutz I, Albrecht U (2010) PERsuading nuclear receptors to dance the circadian rhythm. Cell Cycle 9(13):2515–2521